A Basis for Reduced Chemical Library Inhibition of Firefly Luciferase Obtained from Directed Evolution

Douglas S. Auld,* Ya-Qin Zhang, Noel T. Southall, Ganesha Rai, Marc Landsman, Jennifer MacLure, Daniel Langevin, Craig J. Thomas, Christopher P. Austin, and James Inglese

NIH Chemical Genomics Center, National Institutes of Health, Bethesda, Maryland 20892-3370

We measured the "druggability" of the ATP-dependent luciferase derived from the firefly *Photuris pennsylvanica* that was optimized using directed evolution (Ultra-Glo, Promega). Quantitative high-throughput screening (qHTS) was used to determine IC_{50}s of 198899 samples against a formulation of Ultra-Glo luciferase (Kinase-Glo). We found that only 0.1% of the Kinase-Glo inhibitors showed an $IC_{50} < 10\ \mu M$ compared to 0.9% found from a previous qHTS against the firefly luciferase from *Photinus pyralis* (*lucPpy*). Further, the maximum affinity identified in the *lucPpy* qHTS was 50 nM, while for Kinase-Glo this value increased to 600 nM. Compounds with interactions stretching outside the luciferin binding pocket were largely lost with Ultra-Glo luciferase. Therefore, Ultra-Glo luciferase will show less compound interference when used as an ATP sensor compared to *lucPpy*. This study demonstrates the power of large-scale quantitative analysis of structure–activity relationships (>100K compounds) in addressing important questions such as a target's druggability.

Firefly luciferase has been used to measure ATP concentration, the turnover of pro-luciferin substrates,[1–3] and as a reporter of cell-based gene expression; this has enabled the development of high-throughput screens (HTS) for a wide variety of biological activities. Numerous assays have been developed for protein kinases,[4,5] including measurement of phosphorylated peptide product using solid-phase supports as in SPA[a6] or IMAP[7] as well as recent generic assays for ATPases that employ an ADP-specific antibody.[8–10] Luciferase-coupled assays do not require antibodies or fluorescent labels, thus providing a generic platform for screening that reduces assay development time and reagent costs.[11–13] Therefore, luciferase-based assays remain one of the most ubiquitous technologies for the measurement of ATP concentrations in enzyme assays, particularly kinases—one of the largest, druggable enzyme families that includes sugar, lipid, and protein kinases.[11,12,14] In these assays, the ATP-dependence of firefly luciferase is used to measure the ATP concentration where the luminescence signal is inversely proportional to kinase activity.

A consideration in any assay that uses an enzyme as a reporter or coupled component is inadvertent inhibition of the reporter enzyme by compounds from the library.[5,15–17] Ideally, enzyme reporters would be insensitive to compound inhibition but inhibition of firefly luciferase is commonly observed; both the ATP and luciferin binding sites can be bound by many scaffolds commonly found in compound libraries (e.g.,. benzimidazoles and benzthiazoles). The ATP-dependent luciferase enzyme from the firefly *Photinus pyralis* (*lucPpy*) is employed in several commercial formulations of firefly luciferase used for ATP detection. In a recent profiling screen of approximately 72000 compounds (see PubChem AID: 411) against *lucPpy* contained

in a formulation termed PK-Light (Lonza Corp), we found approximately 3% of this library showed inhibitory concentration–responses, of which 681 (0.9%) exhibited $IC_{50}s < 10\ \mu M$, well within typical compound screening concentration ranges.[15] Investigation of the structure–activity relationships (SAR) of luciferase inhibitors as well as their mode of action revealed classes of luciferin and adenylate competitive compounds as well as large classes of compounds that were noncompetitive with either ATP or luciferin. However, examination of representative compounds from the various inhibitor classes identified in the *lucPpy* qHTS showed that nearly all these were inactive in a luciferase formulation termed Kinase-Glo (Promega Corp). Luciferase assay formulations such as PK-Light and Kinase-Glo all contain high amounts of luciferin (~mM) but lack ATP to allow for sensitive detection of ATP concentration. However, Kinase-Glo differs from other luciferase-based ATP detection formulations in that it contains an optimized luciferase derived from the firefly *Photuris pennsylvanica* (*lucPpe*)[18] known as Ultra-Glo (Promega Corp).[19] Wild-type *lucPpe* and *lucPpy* show 68% similarity.[18] Therefore, one possibility to explain the reduced potency of *lucPpy* inhibitors in Kinase-Glo is that the Ultra-Glo luciferase simply possesses a different SAR and exhaustive profiling of Kinase-Glo would yield a similar number of inhibitors as obtained for the *lucPpy* formulation. Indeed, in our previous study, we observed that small changes in structure (e.g., the addition of a methyl group) showed a marginal increase in Kinase-Glo inhibition ($IC_{50} \sim 10\ \mu M$), supporting the idea that the Ultra-Glo luciferase had an altered SAR. Another possibility is that Ultra-Glo luciferase is genuinely more resistant to inhibitors and thus an analogous qHTS profile would show a reduction in the *lucPpy* inhibitors without a concomitant increase in new inhibitor classes. To explore both the amount and type of compounds associated with inhibition of Ultra-Glo luciferase, we describe here the qHTS of this luciferase against 198899 samples of the MLSMR that included all the compounds assayed previously against the *lucPpy*. The results show a marked *loss* of all inhibitor classes associated with *lucPpy* without a corresponding increase in new inhibitor chemotypes,

---

* To whom correspondence should be addressed. Phone: 301-217-5722. Fax: 301-217-5736. E-mail: dauld@mail.nih.gov.

a Abbreviations: qHTS, quantitative high-throughput screening; *lucPpy*, *Photinus pyralis* firefly luciferase; *lucPpe*, *Photuris pennsylvanica* firefly luciferase; SPA, scintillation proximity assay; Ultra-Glo, optimized variant of *lucPpe* used in Promega's Kinase-Glo formulations; IMAP, immobilized metal-ion affinity partitioning; MSR, minimum significance ratio; CRC, concentration–response curve; BEH, bridged ethyl hybrid.

thus providing evidence that Ultra-Glo luciferase is a more optimal enzyme reporter for ATP detection in HTS. Comparisons of the SAR derived from the qHTS of Kinase-Glo to that previously defined for *lucPpy*,[15] as well as analysis of representative inhibitors, illustrate that the reduced inhibitor susceptibility of Ultra-Glo luciferase is due to a loss of inhibitors whose interactions stretch outside the luciferin pocket including those that likely interact with the adenylate pocket.

Materials and Methods

Reagents. ATP, BSA, Tween 20, potassium chloride, imidazole, D-luciferin, and the luciferase control compound **1** (SIB 1757)[20] were purchased from Sigma-Aldrich. Magnesium chloride was acquired from Quality Biological, and dimethylsulfoxide (DMSO), certified ACS grade, was purchased from Fisher. The Ultra-Glo luciferase-based detection reagents used were Kinase-Glo, Kinase-Glo Plus, and Kinase-Glo Max (Promega; Madison, WI). Purified wild-type *lucPpy* luciferase was obtained from Sigma (cat. no. L9506) and purified Ultra-Glo luciferase was obtained from Promega.

Preparation of Compound Libraries and Control Plates. The 198899 member library was collected from several sources: 185021 compounds from the NIH MLSMR,[21] 1280 compounds from Sigma-Aldrich (LOPAC1280), 1120 compounds from Prestwick Chemical Inc., 361 purified natural products from TimTec (Newark, DE), three 1000-member combinatorial libraries from Pharmacopeia (Princeton, NJ), libraries that include pharmacologically active compounds such as opioids, adrenergics, cholinergics, serotonergics, dopaminergics, histaminergics, and endocannabinioids from Tocris (1105 compounds; Ellisville, Missouri), Biomol (256 compounds; Plymouth Meeting, PA), Spectrum (1952 compounds; Gardena, CA), as well as 198 compounds synthesized at the NCGC, 1957 compounds from the National Cancer Institute, 48 nucleoside and nucleotide-based compounds from Biolog Life Science Institute distributed by Axxora LLC (San Diego, CA) and from various Centers for Chemical Methodology and Library Development, including 47 from the University of North Carolina, 81 from Texas A&M University, 96 from the University of Wisconsin, 252 from University of Pittsburgh, 989 from the University of Pennsylvania, and 1136 compounds from Boston University. Interplate dilutions of the libraries were prepared as described.[22,23]

Controls were added from a separate 1536-well compound plate as follows: columns 1 and 2, 16-point titrations in duplicate of ATP and the control inhibitor **1**, respectively (both beginning at 10 mM in DMSO); column 3, the neutral control (DMSO); column 4, the control inhibitor (10 mM in DMSO).

Luciferase Assay and qHTS. First, 4 μL/well of substrate/buffer (10 μM ATP, 50 mM KCl, 7 mM MgCl$_2$, 0.05% BSA, 0.01% Tween 20, and 50 mM imidazole pH 7.2, final concentration) was dispensed into Kalypsys solid white 1536-well plates using a bottle-valve solenoid-based dispenser (Kalypsys). Then 23 nL of compound solution was transferred to the assay plate using a Kalypsys pin tool equipped with a 1536-pin array[24] containing 10 nL slotted pins (FP1S10, 0.457 mm diameter, 50.8 mm long; V&P Scientific). Following transfer, 2 μL/well of Kinase-Glo was dispensed for a final assay volume of 6 μL/well. Following an 8 min incubation at ambient temperature, luminescence was detected by a ViewLux (Perkin-Elmer) using a 5 s exposure time and 1× binning. All screening operations were performed using a fully integrated Kalypsys robotic system containing one RX-130 and two RX-90 Staübli anthropomorphic robotic arms.[25]

qHTS Data and SAR Analysis. Screening data was processed using in-house developed software. Percent activity was computed from the median values of the uninhibited, or neutral, control (32 wells located in column 3) and the 40 μM of **1**, or 100% inhibited, control (32 wells, column 4), respectively. For assignment of plate concentrations and sample identifiers, ActivityBase (ID Business Solutions Ltd., Guildford, UK) was used for compound and plate registrations. An in-house database was used to track sample concentrations across plates. Correction factors were generated from

33 control assay plates containing vehicle (DMSO) only that were inserted uniformly throughout the screen to monitor background systematic variation in assay signal. Curve fitting was performed using an in-house developed algorithm (a version of which is available online).[26] Curve-fitting and SAR analysis was performed as described,[15,22] where the noise of the assay was estimated by calculating the standard deviation (SD) of the activity values obtained at the lowest tested compound concentration and outliers were identified and masked by modeling the Hill equation and determining if the differences exceeded the assay noise. The qHTS data was depicted using Origin (OriginLab). Data have been deposited in PubChem (AID 1379).

Synthesis of 2-Phenylbenzothiazole Compounds. To a mixture of 2-bromobenzo[*d*]thiazole or 2-bromo-6-methoxybenzo[*d*]thiazole (0.25 mmol) and selected arylboronic acids/boronates (0.325 mmol) in 2 mL of DME in a microwave tube (2–5 mL capacity) was added Pd(PPh$_3$)$_4$ (5 mol %, 0.012 mmol) and a 2.0 M aqueous solution of K$_2$CO$_3$ (0.25 mmol). The mixture was irradiated with MW for 5–45 min at 150 °C, cooled, diluted with 25 mL of ethyl acetate, and filtered through celite. The solvent was evaporated, and the crude material was purified on a Biotage silica gel column. Gradient elution with ethyl acetate in hexanes (proportions changed based upon the R_f value of the products) gave the coupled products as solids.

Analytical QC of Compounds. The entire library was subjected to purity analysis before plating (Galapagos Biofocus DPI, South San Francisco, CA). Active compounds that were obtained from commercial sources were reanalyzed for purity. For these resupplied compounds, the purity analysis was performed via LCMS analysis on a Waters ACQUITY reverse phase UPLC System and 1.7 μm BEH column (2.1 mm × 50 mm) using a linear gradient in 0.1% aqueous formic acid (5% ACN in water increasing to 95% over 3 min). Compound purity was measured based upon peak integration from both UV/vis absorbance and ELSD, and compound identity was based upon mass analysis; all compounds passed purity criteria (>95%). See Supporting Information for proton and high-resolution mass spectral data of selected compounds.

Follow-up Luciferase Assays. A total of 39 compounds were obtained and subjected to several luciferase assays using a 1536-well plate format. Purified firefly luciferases were assayed in a buffer containing 50 mM Tris-Acetate pH, 10 mM Mg-acetate, 0.01% Tween, 0.05% BSA, 10 μM D-luciferin, 10 μM ATP, and luciferase at 10 nM. Alternatively, this same buffer and enzyme concentration was used to vary either D-luciferin or ATP concentrations to determine K_M or concentration–response curves (CRCs). For assaying Kinase-Glo, Kinase-GloPlus, or Kinase-GloMax, the same buffer used in the qHTS was used. Luminescence was collected on the Perkin-Elmer Viewlux. Each compound was assayed in duplicate and this experiment repeated on two or three separate days.

Results

Luciferase qHTS. We used a commercially available detection system containing Ultra-Glo luciferase, luciferin, and buffer components (Kinase-Glo) for the screen. This system showed linear performance of enzyme activity through a range of 2–10 μM of ATP in a manner similar to the *lucPpy* contained in PK-Light for which the previous qHTS was performed,[15] supporting similar sensitivity to ATP between the two enzymes. Therefore, identical buffer systems containing 10 μM ATP and high (~50 × K_M) concentrations of luciferin could be used for both qHTS studies. The screen was performed in 1536-well plate format with a final assay volume of 6 μL per well. Compound **1** (Figure 1), identified as an inhibitor of Ultra-Glo luciferase in our previous study, was used as an inhibitor control.

The Ultra-Glo luciferase activity was screened against approximately 199K compounds using qHTS, where the activity is measured across multiple concentrations allowing the generation of CRCs for all library compounds.[22] In the luciferase
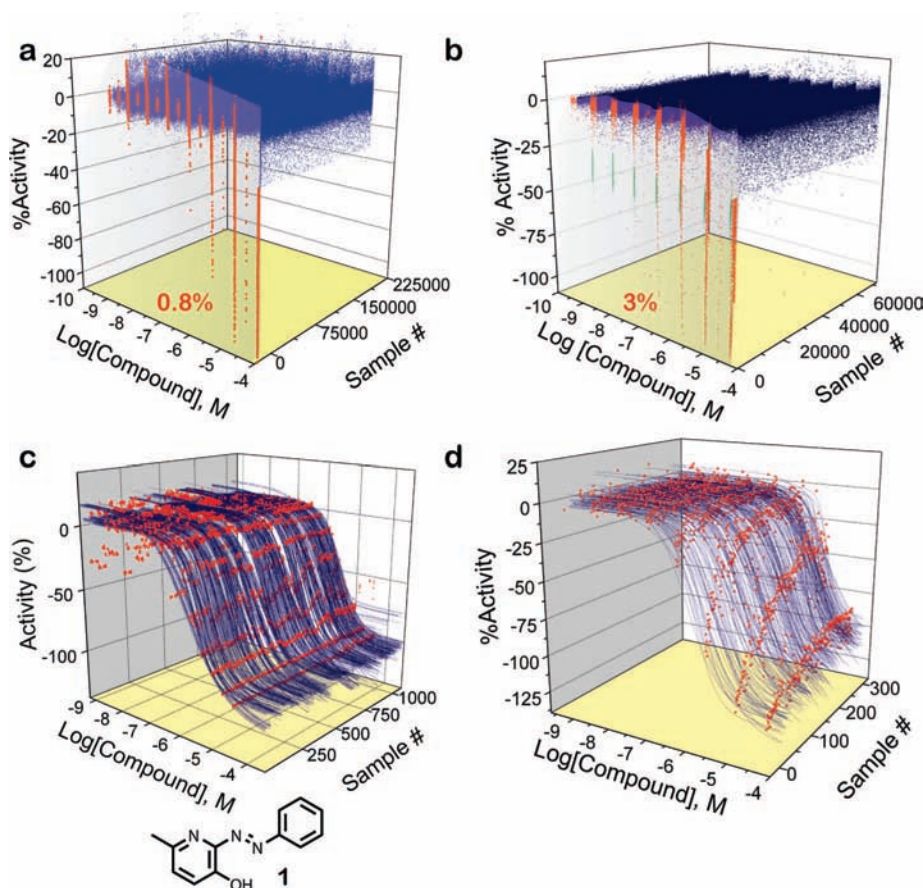
Figure 1. Summary of the qHTS. (a) Results of the Ultra-Glo luciferase qHTS. Concentration−response data are shown for active (red; percentage of actives noted) and inactive (blue) compounds. (b) Results of the previous qHTS using the *lucPpy* formulation[15] is shown for comparison. Activities for 352 compounds (green) in the *lucPpy* qHTS were reduced because of a partially blocked tip. Percentage of actives noted in red. (c) Control inhibitor (**1**) titration response curves and structure of **1** are shown. (d) Representation of class 1a, 1b, and 2a CRCs derived from the Ultra-Glo luciferase qHTS. Data points are shown in red with the fitted CRC curves shown in blue.

qHTS, the library was tested as a series of at least seven 5-fold dilutions at a beginning concentration of approximately 40 μM.

A total of 1088 1536-well microtiter plates were processed. The assay showed an average signal-to-background ratio = 8.1 ± 2.9 and $Z' = 0.74 \pm 0.13$, indicating a performance that was comparable to the previous qHTS against *lucPpy* (Figure 1a,b). The inhibitor control titrations included on every plate were highly precise as judged by the minimum significance ratio (MSR)[27] for compound **1** that was calculated to be $1.89_{n = 1088}$ (Figure 1c).

The qHTS resulted in titration-response profiles of 198899 samples derived from approximately 1.53 million assayed wells (Figure 1b). The screen was performed using an optimized 1536-well protocol (Table 1) so that one CRC was generated per second on the Kalypsys automated system.[25] Automated curve-fitting was performed to generate CRC fits to the data corresponding to each sample. The CRCs were then separated into four classes: (1) complete CRCs containing upper and lower asymptotes, (2) incomplete CRCs having an upper asymptote, (3) poorly fit CRCs or where the activity was observed only at the highest tested concentration, and (4) inactive where activity of all unmasked data points was below 30%. Each CRC class was further divided based on the efficacy of response (e.g., CRC classes "1a, 1b"; see Inglese et al.[22]).

The screen identified 0.78% of the library samples as active (class 1−3). The distribution of potencies within each CRC class is summarized in Table 2. Compounds associated with the highest quality CRCs, Class 1a, 1b, and 2a, comprising 43, 11,

Table 1. Final 1536-Well Assay Protocol

step[a]	parameter	value	description
1	reagent, μL	4	10 μM ATP buffer
2	library compounds, nL	23	40 μM to 0.24 nM dilution series
3	controls, nL	23	ATP, compound **1**, DMSO
4	reagent, 2 μL		detection buffer
5	incubation time, min	8	RT incubation
6	assay readouts	5	luminescence read

[a] Step Notes: (1) Medium-binding white solid Kalypsys plates. 100 μL pre-dispense, four-tip dispense columns 1−48. Buffer: 50 mM KCl, 7 mM MgCl$_2$, 10 μM ATP, 0.01% Tween, 0.05% BSA. Mixture kept on ice. (2) Pin-tool transfer compound library for a (final) range of 40 μM to 0.24 nM. (3) Pin-tool transfer, column 1 16-point titrations in duplicate of ATP beginning at 10 μM (final), column 2, 16-point titrations in duplicate of compound **1** beginning at 40 μM (final), column 4, compound **1** at 40 μM (final). Pin-tool transfer tip wash sequence: DMSO,iPA, MeOH, 3 s vacuum dry. (4) Kinase-Glo reagent containing Ultra-Glo luciferase and high concentrations (∼mM) of luciferin. 100 μL pre-dispense, four-tip dispense columns 1−48. (5) RT incubation in auxilliary plate hotel. (6) PE ViewLux, clear filter.

and 232 samples, respectively, represented 0.15% of the collection (Figure 1d; Table 2). Class 2b was the largest class of actives, containing 837 samples (0.4%), while class 3 totaled 413 samples (0.2%). Class 1 CRCs spanned a potency range from 0.6 to 10 μM and included the positive control compound **1** that was present within the Tocris library. In contrast, the maximum inhibitor potency obtained in the *lucPpy* qHTS was 50 nM. Potencies for class 2a and 3 should be considered approximations as they are extrapolated from incomplete CRCs.

Table 2. Analysis of qHTS. Numbers in parenthesis represent the % of inhibitors found for this CRC class in the *lucPpy* qHTS

IC$_{50}$ (μM)	curve classification					
	1a	1b	2a	2b	3	total
<0.1	0	0	0	0	0	0
0.1−1	3	11	0	0	0	14
1−10	40	0	139	335	159	673
10−100	0	0	93	502	254	849
total per classification	43	11	232	837	413	1,536
% of Library	0.02, (0.29)	0.01, (0.19)	0.12, (0.34)	0.42, (1.79)	0.21, (0.59)	0.78, (3.19)

Comparison of Activity between lucPpy and Ultra-Glo Luciferase. For the *lucPpy* qHTS we observed that 3.1% of the library samples were active (class 1−3),[15] whereas only 0.9% of the samples were active in the Ultra-Glo luciferase qHTS. Potent inhibitory compounds showing high quality CRCs were dramatically reduced in Ultra-Glo luciferase compared to the *lucPpy* formulation as only 0.15% of compounds in the Ultra-Glo luciferase qHTS had a CRC class 1a, 1b, or 2a CRC versus 0.82% for *lucPpy* qHTS (Table 2). Additionally, we found only 0.03% Class 1 CRCs in Ultra-Glo luciferase, while 0.48% was found within this CRC class using the *lucPpy* formulation (Table 2). Further, of the class 1 CRCs from the *lucPpy* luciferase qHTS 50% were found as inactive (class 4) in the Ultra-Glo luciferase qHTS.

The potency distribution between the qHTS against Ultra-Glo and *lucPpy* luciferase is summarized in Figure 2. Only 0.1% of the Ultra-Glo luciferase inhibitory compounds showed an IC$_{50}$ < 10 μM compared to 0.9% using the *lucPpy* formulation. Overall, the Ultra-Glo luciferase qHTS showed an average potency that is 7-fold weaker than what was found in the *lucPpy* qHTS.

Characterization of Selectivity between Ultra-Glo and lucPpy Luciferases. We have identified several prominent scaffolds that act as luciferase inhibitors, including several luciferin mimetic compounds such as those containing a benzothiazole core.[15] The same chemical series were again identified in the Ultra-Glo luciferase screen but with greatly reduced activity (Figure 3). In general, there was a marked loss of inhibitors containing benzoxazole (**4**), benzthiazole (**5**), or benzimidazole (**6**) cores (reduced by 93%, 80%, and 76%, respectively; Figure 3) that likely bind at luciferyl-adenylate pocket of luciferase. We also noted that a potent inhibitor class containing a 3,5-diaryl-oxadiazole core (**2**, Figure 3), where we
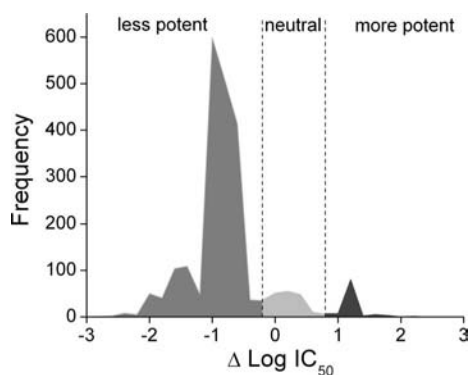

Figure 2. Difference in potency distribution between *lucPpy* and Ultra-Glo luciferase formulations. Active compounds from the previous *lucPpy* qHTS and the Ultra-Glo luciferase qHTS were compared and the ΔLogAC$_{50}$ values were calculated. Negative ΔLogAC$_{50}$ values represent compounds that were less potent in the Ultra-Glo luciferase compared to the *lucPpy* qHTS, while positive ΔLogAC$_{50}$ values represent compounds that were more potent in the Ultra-Glo luciferase compared to the *lucPpy* qHTS.

have found that the inhibition cannot be completely relieved by addition of high substrate concentrations, was also reduced but to a lesser extent (60% reduction). Similarly, the number of active compounds in the benzamide class (**3**, Figure 3) was reduced by 80% in the Ultra-Glo luciferase qHTS.

To investigate the reason for the reduced inhibitor fraction in the Ultra-Glo luciferase qHTS experiments, we obtained represented compounds and characterized these against purified Ultra-Glo luciferase and *lucPpy*. We also measured activity of these compounds in several commercial preparations of Ultra-Glo luciferase.

To explore the luciferin binding pocket, we examined 22 2-phenylbenzothiazole (**7**) analogues against the two luciferases (Table 3). These compounds represented minimal luciferin mimetic analogues and were generally either unsubstituted or contained simple halogen or methyl group substitutions. We determined similar potency values for these compounds using either purified Ultra-Glo luciferase or *lucPpy* and K$_M$ levels of substrates against this series of analogues (Table 3). Therefore, the specificity within the luciferin pocket is similar between the two luciferases. Consistent with competitive behavior, we also noted that all these compounds showed greatly weakened inhibition or became inactive in the commercial Ultra-Glo luciferase-containing reagents that contain excess luciferin substrate (Table 3).

However, we noted that a 4-(6-methoxybenzo[d]thiazol-2-yl)-*N,N*-dimethylaniline (**7p**) showed nearly 4-fold weaker potency against purified Ultra-Glo luciferase than *lucPpy* and this compelled us to examine additional analogues (**7a−7x**; Table 3) at the 2-position of the benzothiazole that incorporated larger substitutions. For this purpose, we examined the potency of several analogues under a range of luciferin and ATP concentrations (Figure 4) using purified Ultra-Glo and *lucPpy* luciferases. Further we compared **7p** as well as two analogues that contained a larger pyrazole-containing substitution to representative analogues mentioned above that contained simple halogen substitutions (e.g., **7d**, **7e**, and **7f**). We found that the halogen substituted analogues behaved as pure luciferin competitive inhibitors with substrate variation, showing similar effects between the two luciferases (Figure 4a−c). However, **7p** and two compounds containing a 1-benzyl-1*H*-pyrazole at the 2-position (Figure 4; **7w** and **7x**) showed different substrate dependences for the two luciferases. In the case of Ultra-Glo luciferase, these compounds remained largely luciferin competitive as shown by the general loss of activity at high luciferin concentrations (Figure 4d−f). However, for *lucPpy*, these compounds showed greater potency for *lucPpy* than Ultra-Glo luciferase upon either luciferin or ATP variation (compare red and black fits, Figure 4e,f). In the qHTS, D-luciferin was present in large excess in both the Ultra-Glo and *lucPpy* luciferase formulations and we measured only a 4-fold higher affinity K$_M$ for luciferin with Ultra-Glo luciferase than *lucPpy* (0.9 ± 0.1 vs 4 ± 0.4 μM, respectively). Therefore, changes in substrate affinity alone cannot explain the large loss of these inhibitory
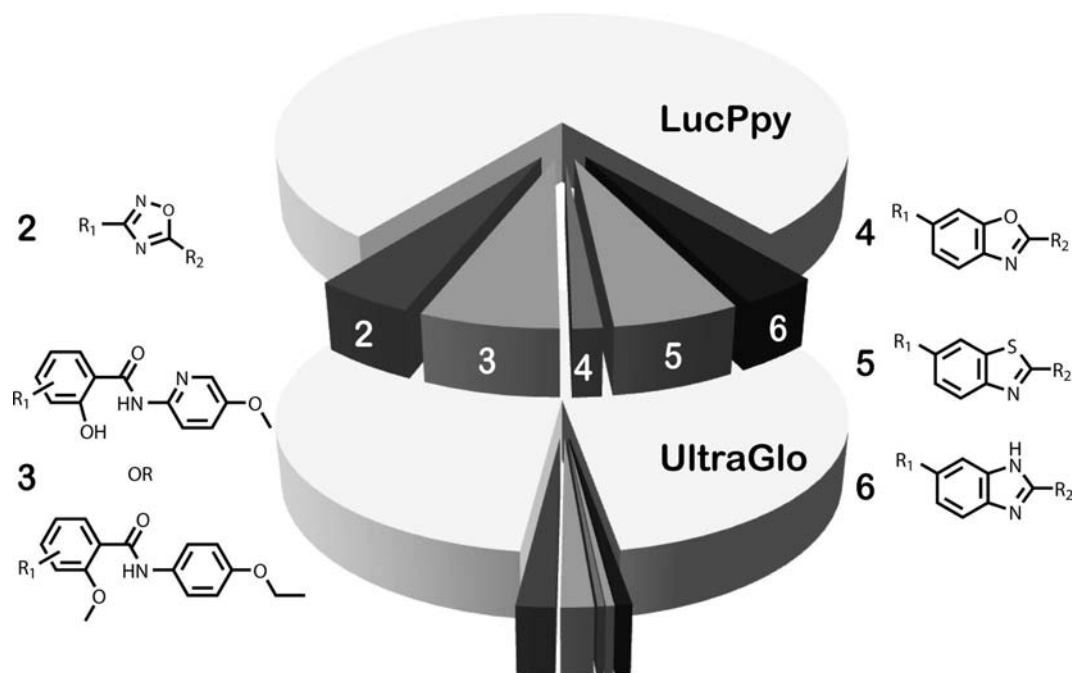
Figure 3. Comparison of inhibitor scaffold representation between *lucPpy* and Ultra-Glo luciferase formulations. Center pie charts represent the amount of active (darker gray slices) and related inactive analogues (light-gray area in each pie chart) for prominent luciferase inhibitor scaffolds (**2–6**) for the *lucPpy* (top pie) and Ultra-Glo luciferase (bottom pie) qHTS. The scaffolds and the associated analogues were determined as described in Auld et al.[15] The number of *lucPpy* active analogues was reduced from 70 to 27 (**2**, 3,5-diaryl-oxadiazoles), 98 to 23 (**3**, benzamides), 21 to 5 (**4**, benzoxazoles), 89 to 6 (**5**, benzthiazoles), and 55 to 11 (**6**, benzimidazoles) in the Ultra-Glo luciferase qHTS. The corresponding number of structurally related inactive analogues increased from 1192 to 1442 in the Ultra-Glo luciferase qHTS.

Table 3. Characterization of Selected 2-Phenylbenzothiazole Analogues[a]

| analogue no.	R_1	R_2	R_3	R_4	$IC_{50 UltraGlo}$	$IC_{50 lucPpy}$	$IC_{50 KinGlo}$	$IC_{50 KinGlo\ Plus}$	$IC_{50 KinGlo\ Max}$
a	H	H	H	dimethylamine	0.32 ± 0.0	0.2 ± 0.0	10.7 ± 3.4	inactive	inactive
b	H	H	H	Cl	1.4 ± 0.18	4.5 ± 0.0	>50	inactive	inactive
c	OMe	H	H	F	0.86 ± 0.08	1.3 ± 0.09	>50	inactive	inactive
d	OMe	H	F	H	1.1 ± 0.14	1.5 ± 0.1	>50	inactive	inactive
e	OMe	F	H	H	0.5 ± 0.05	0.6 ± 0.0	>50	inactive	inactive
f	OMe	Cl	H	F	4.9 ± 1.1	5.4 ± 0.7	>50	inactive	inactive
g	OMe	H	H	Cl	3.8 ± 0.5	3.5 ± 0.0	>50	inactive	inactive
h	OMe	*O*-methylbenzene	H	H	4.3 ± 0.2	8.9 ± 0.6	>50	inactive	inactive
i	OMe	H	*O*-methylbenzene	H	30 ± 3	13.4 ± 1	inactive	inactive	inactive
j	OMe	H	H	CN	6.1 ± 1.3	5.7 ± 0.9	inactive	inactive	inactive
k	OMe	H	H	OMe	4.1 ± 0.4	2.2 ± 0.0	>50	inactive	inactive
l	OMe	OMe	H	H	5.6 ± 1.3	3.2 ± 0.0	>50	inactive	inactive
m	OMe	H	OMe	OMe	3.8 ± 0.6	2.8 ± 0.0	>50	inactive	inactive
n	OMe	H	acetamide	H	1.9 ± 0.4	2.9 ± 0.2	>50	inactive	inactive
o	OMe	H	Me	H	0.67 ± 0.07	1.5 ± 0.1	>50	inactive	inactive
p	OMe	H	H	dimethylamine	2.7 ± 0.6	0.7 ± 0.04	>50	inactive	inactive
q	H	H	F	H	7.8 ± 0.3	24.2 ± 1.6	inactive	inactive	inactive
r	H	H	OMe	OMe	1.9 ± 0.3	3.2 ± 0.0	>50	inactive	inactive
s	H	H	H	OMe	0.36 ± 0.02	1.0 ± 0.0	>50	inactive	inactive
t	H	OMe	H	H	7.7 ± 1.4	11.3 ± 1.8	>50	inactive	inactive
u	H	H	H	CN	2.1 ± 0.2	6.3 ± 0.0	>50	inactive	inactive
v	H	H	H	acetamide	3.1 ± 0.5	3.0 ± 0.2	>50	inactive	inactive

[a] Activity of compounds was determined by measurement of luminescence using either purified luciferase enzyme assays ($IC_{50 UltraGlo}$ or $IC_{50 lucPpy}$) or formulations of UltraGlo ($IC_{50 KinGlo}$, $IC_{50 KinGlo\ Plus}$, $IC_{50 KinGlo\ Max}$). Data shown are mean ± SD for at least three replications.

classes in the qHTS, rather a shift to a noncompetitive luciferin binding mode due to interactions outside the luciferase pocket appears to result in more prevalent inhibitors for *lucPpy* formulations.

To further test possible reasons for this selectivity, we examined the potencies at Ultra-Glo luciferase for a series of quinoline compounds identified in the *lucPpy* qHTS that were shown to be competitive with ATP and luciferin and modeled into the adenylate binding pocket of firefly luciferase.[15] Consistent with this pocket serving as a mediator of selectivity between the two luciferases, we found a marked loss of activity for these quinolines for Ultra-Glo luciferase (Figure 5). Two of the most potent quinolines for *lucPpy* were **8** (Figure 5, *lucPpy* $IC_{50} = 0.5\ \mu M$) and **9** (Figure 5, *lucPpy* $IC_{50} = 4.0\ \mu M$). Both **8** and **9** showed IC_{50}s >10 μM, outside the typical screening concentration range, against Ultra-Glo luciferase (Figure 5).
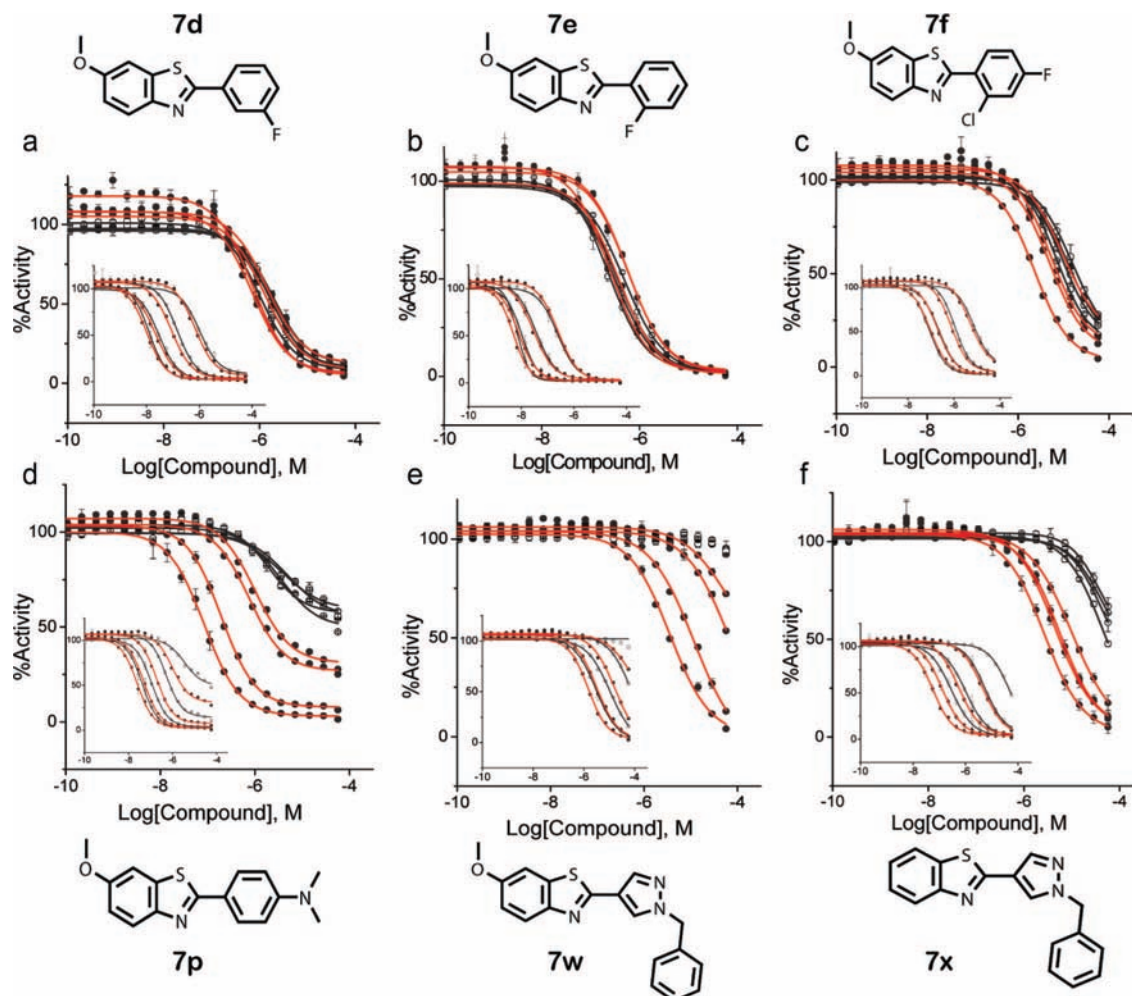
Figure 4. Comparison *lucPpy* and Ultra-Glo luciferase against 2-phenylbenzothiazole luciferase inhibitors at multiple substrate concentrations. Graphs of ATP variation or luciferin variation (inset) are shown. Luciferin or ATP was varied at 0.25, 2, 25, and 250 μM, resulting in four sets of CRCs. In each case, the constant substrate was present at 250 μM. The *lucPpy* data is shown as solid circles with red CRC fits, and the Ultra-Glo luciferase is shown as open circles with black fitted lines. The structures of the inhibitors assayed are also shown. The top graphs show compounds with luciferin competitive behavior against both *lucPpy* and Ultra-Glo luciferase, while the bottom graphs demonstrate inhibitors that maintain potency at high ATP or luciferin concentrations for *lucPpy* but not Ultra-Glo luciferase.

Further, in formulations of Ultra-Glo luciferase, this series is inactive. This suggests that favorable interactions within the adenylate pocket are present in *lucPpy* that are absent in Ultra-Glo luciferase, suggesting the adenylate pocket as one of the regions that determines the large reduction in the inhibitors for Ultra-Glo luciferase.

Compounds that show a noncompetitive behavior against reporter enzymes used in HTS, perhaps by exploring inhibitory sites outside the active site, will be more of a nuisance as the inhibition will not be completely relieved by increasing substrate concentrations. Our previous work identified the 3,5-diaryl-oxadiazoles as potent noncompetitive inhibitors against *lucPpy*[15] and indeed some of the most potent compounds identified here contained a 3,5-diaryl-oxadiazoles core (**2a**−**l**; Table 4). Of these, the most potent compounds showed IC$_{50}$s $\sim$ 50 nM at low substrate concentrations but showed reduced potencies near 10 μM in the formulated reagents (e.g., **2d,e**). Although this inhibitor class also showed a large reduction of inhibitory compounds ($\sim$60% less) in the Ultra-Glo luciferase qHTS, we noted that the 3,5-diaryl-oxadiazoles series was the one compound series that still contained a significant number of compounds, which demonstrated appreciable inhibition in

formulations of Ultra-Glo luciferase such as Kinase-GloPlus and Kinase-GloMax (Table 4).

Discussion

We have determined a comprehensive inhibitor profile of $\sim$199K compounds using an optimized formulation of Ultra-Glo luciferase and compared this to a previously determined inhibitor profile that used an analogous *lucPpy*-containing formulation.[15] The Ultra-Glo luciferase formulation (Kinase-Glo) showed reductions in both inhibitor abundance and potency relative to *lucPpy* with only 0.1% of library showing IC$_{50}$ <10 μM in the Ultra-Glo luciferase formulation compared to 0.9% with the *lucPpy* formulation. Although we noted similar specificity for compounds purely competitive with luciferin substrate, we found that one of the principle reasons for the lower number of inhibitors against Ultra-Glo luciferase was due to a loss of compounds with interactions stretching outside the luciferin pocket. These interactions allow for inhibition to persist even at high D-luciferin for *lucPpy*, while the absence of these interactions renders these inhibitors inactive in Ultra-Glo luciferase formulations. Therefore, formulations such as Kinase-Glo should be superior ATP sensor reagents for HTS, as these will have lower compound interference. Indeed, a previous study
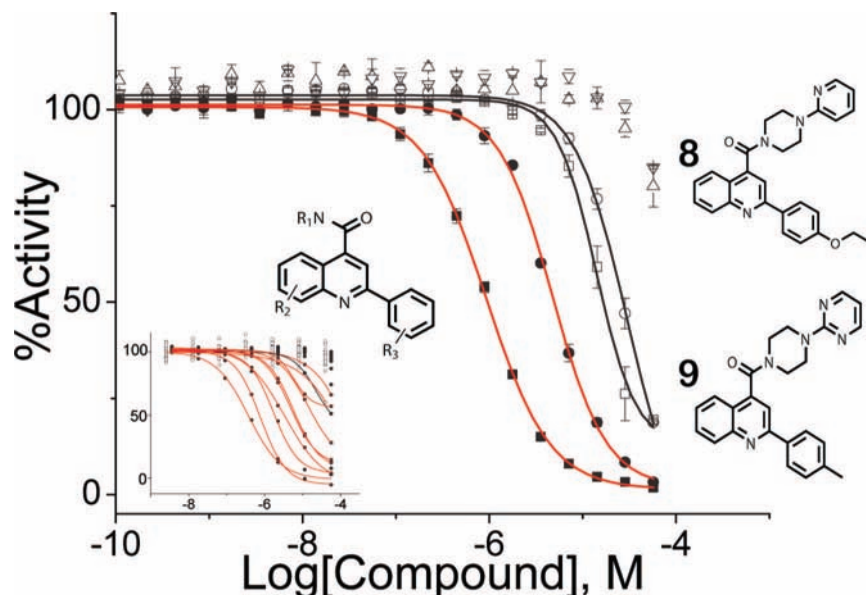
Figure 5. Comparison of *lucPpy* and Ultra-Glo luciferase inhibition for a series of quinoline analogues. Red fits, solid circles and squares are *lucPpy*, and black fits, open circles, and squares are Ultra-Glo luciferase for **8** (squares) or **9** (circles) assayed using K_M levels of substrates. Also shown is the activity of these two compounds using Kinase-Glo for **8** (open triangles) and **9** (upside-down open triangles). The inset shows activity in the qHTS for a series of related quinolines in the *lucPpy* qHTS (solid circles, red-fits) and Kinase-Glo (open circles).

Table 4. Characterization of Selected 3,5-diaryl-oxadiazoles from the qHTS[a]
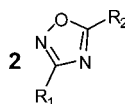
analogue no.	R_1	R_2	$IC_{50UltraGlo}$	$IC_{50P.Pyralis}$	$IC_{50KinGlo}$	$IC_{50KinGlo\ Plus}$	$IC_{50KinGlo\ Max}$
a	pyridin-2yl	pyridin-4yl	1.9 ± 0.6	14.4 ± 6.9	8.9 ± 1.9	14.1 ± 0.0	25.3 ± 4.1
b	pyridin-2yl	furan-2yl	1.3 ± 0.3	17.1 ± 7.1	13.9 ± 0.6	>50	>50
c	pyridin-2yl	biphenyl-4yl	0.038 ± 0.006	0.08 ± 0.07	11.3 ± 1.7	>50	>50
d	pyridin-2yl	4-phenyl benzoate	0.040 ± 0.006	1.4 ± 1.2	10.0 ± 3.4	13.4 ± 2.4	13.1 ± 2.5
e	pyridin-2yl	2-methoxy phenyl	0.08 ± 0.01	2.8 ± 1.6	5 ± 1	13.5 ± 0.8	12.7 ± 1.7
f	phenyl	2,4-dimethoxy phenyl	0.054 ± 0.004	0.2 ± 0.1	13.9 ± 1.1	>50	>50
g	3-methyl phenyl	4-flouro phenyl	0.58 ± 0.1	1.7 ± 0.5	14 ± 7.7	inactive	inactive
h	4-methoxy phenyl	2-flouro phenyl	0.3 ± 0.05	2.8 ± 1.6	>50	>50	inactive
i	2-methoxy phenyl	phenyl	0.6 ± 0.1	8.3 ± 3.7	>50	inactive	inactive
j	2-methoxy phenyl	pyridin-4yl	4.8 ± 0.7	24 ± 9.8	>50	inactive	inactive
k	pyridin-4yl	furan-2yl	2.4 ± 0.3	24 ± 10.7	>50	inactive	inactive
l	4-dimethyaminophenyl	2-methoxy phenyl	0.32 ± 0.04	0.5 ± 0.3	inactive	inactive	inactive

[a] Activity of compounds was determined by measurement of luminescence using either purified luciferase enzyme assays ($IC_{50UltraGlo}$ or $IC_{50lucPpy}$) or formulations of UltraGlo ($IC_{50KinGlo}$, $IC_{50KinGlo\ Plus}$, $IC_{50KinGlo\ Max}$). Data shown are mean $\pm$ SD for at least three replications.

that used Kinase-Glo for HTS of glycogen synthase kinase-3 noted that no luciferase inhibitors were identified during confirmation of the primary hits.[28]

Although Ultra-Glo luciferase formulations appear to be more optimal assay reagents for ATP detection in HTS, we note that Ultra-Glo luciferase reagents intended for uses other than ATP detection, where luciferin concentrations may be present at lower concentrations, could contain additional inhibitors than described here. For example, given the potent binding for many inhibitors we found using low luciferin concentrations, certain reagents containing pro-luciferin substrates[3] will likely show increased amounts of luciferase inhibitors compared to the profile described here. The potent inhibition of firefly luciferases by luciferin competitive compounds in unformulated reagents should also caution against the temptation to dilute detection reagents further than supplier suggestions to save costs. Even though diluted detection reagents can show adequate signal: background, increased interference by luciferase inhibitors will be obtained.

The Ultra-Glo luciferase was derived from *lucPpe* and was optimized by directed evolution[19,29,30] using a selection strategy that incorporated several steps and introduced as many as 34 mutations. This included screening for variants of increased thermostability, signal stability ("glow response"), substrate usage efficiency through evaluation of K_M values, and increased inhibitor resistance. Inhibitor resistance was determined by adding L-luciferin into the reaction mix and selecting for variants that were resistant to this inhibitor[29] because studies have shown that L-luciferin can act as a competitive inhibitor of the bioluminescent reaction; the enantiomeric position of luciferin being the site of adenylate attachment.[31,32] Some of the mutations introduced in this process were found to improve the K_M for ATP (from 18 μM to approximately 3 μM, relative to wild-type *lucPpe*),[29] consistent with changes in the adenylate pocket and may have improved the resistance to inhibitors.

Firefly luciferase is a globular protein composed of N- and C-terminal domains linked by a hinge region. These two domains are known to undergo a change upon substrate binding

that brings the two domains together, resulting in a more compact closed conformation.[33,34] The final thermostable Ultra-Glo luciferase variant showed a half-life of more than 100 days at room temperature, representing an improvement in half-life at 50 °C of approximately 5000-fold over unoptimized *lucPpe*.[29] Additionally, the increased thermostability of Ultra-Glo luciferase may have led to increased conformational rigidity, resulting in a relatively more compact closed conformation, thus blocking many of the small molecule binding sites present in unoptimized *lucPpy*. Indeed, comparison of protein structures between hyperthermophilic and mesophilic organisms shows increased hydrophobic packing and decreased flexibility in the hyperthermophilic proteins.[35,36]

Observing a difference in druggability between related enzymes is not without precedence[37,38] and a similar mechanism involving conformational flexibility has been proposed to explain druggability differences in protein kinases. In the cocrystal of Raf protein kinase in complex with 4-(4-(3-(4-chloro-3-(trifluoromethyl)phenyl)ureido)phenoxy)-*N*-methylpicolinamide (Bay 43-9006),[39] the compound is found to bind to a large open binding pocket present in the inactive state of the ATP pocket, thus leading to inhibition through stabilization of the inactive conformation of the kinase.[40] However, in the protein kinase Tie2, this binding site is closed because it is filled by the nucleotide binding loop that prevents small molecule inhibition.[41] Therefore, conformational flexibility and relative plasticity have been proposed to explain why certain targets are associated with many inhibitor scaffolds while others have been resistant to efforts to develop inhibitors and may represent another reason for the improved resistance to inhibitors for Ultra-Glo luciferase.[42,43]

Methods aimed at understanding target druggability are of great interest as these can lead to better choices of targets geared for small molecule intervention. The term "druggability" has been defined as the ability to identify high affinity and selective small (e.g. ∼500 MW) druglike compounds that show tractable SAR against a molecular target.[38,44,45] Understanding target druggability has been approached through various methods in the past, including computational methods employing sequence alignment information or crystal structures.[45,46] A recent study used an affinity model to predict druggability where an experimental HTS against 11K compounds was performed to confirm the results.[46] In that study, it was shown that a target predicted to have low druggability, and for which researchers at Pfizer were unable to identify suitable leads after considerable effort, showed a 90% reduction in hits compared to a target predicted to have high druggability. As well, the maximum achievable potency was predicted to be 10-fold higher for the druggable target. These metrics are in line with the experimental results obtained here as we also observed a 90% reduction in major inhibitor classes and a 10-fold reduction in the maximum observed potency when comparing the two luciferase qHTS experiments, supporting that Ultra-Glo luciferase reagents are less "druggable".

Current technologies allow for rapid determination of potency values across large chemical libraries in a manner in which robust SAR is experimentally measured for the entire library. Such an experiment employed early in the drug discovery process where both the maximum inhibitor potency and fraction of active compounds is directly determined could save unnecessary time and effort on intractable target classes. However, an alternative reason for the reduced inhibitor fraction found here for Ultra-Glo luciferase could be that the MLSMR, which contains largely small molecule druglike compounds, does not

contain the right structures for high affinity binding to Ultra-Glo luciferase. A recent study describing a screen of sphingosine 1-phosphate (S1P) receptors against the MLSMR suggested that chemical library biases may have played a role in the determining different hit rates between two S1P receptor subtypes.[47] Further expansion of the qHTS approach to other target classes and different types of chemical libraries (e.g., natural products) will provide experimental testing that can be used to determine how the nature of the library affects the hit rate of the target class. The qHTS database already established at our center and available within PubChem[21] could be mined to obtain such information for relevant target classes.

Given the wide use of enzyme-based reporters in the early phases of compound discovery efforts, it would seem wise to critically examine the mechanisms of inhibition of these common reporter enzymes. This knowledge can be used to distinguish the SAR related to the targeted biology versus reporter specific effects that can result in misleading activity. For example, using our understanding of firefly luciferase inhibitor SAR, we have recently demonstrated that inhibition of firefly luciferase in cell-based reporter assays can lead to the counter-intuitive phenomena of apparent reporter gene activation due to inhibitor-based stabilization of the reporter enzyme within the cellular milieu.[16] Assay interferences due to inhibition of reporter enzymes such as firefly luciferase offer the opportunity to understand the SAR in "medicinal chemistry" terms, and this knowledge can be used to ensure proper interpretation of the results and use of this important bioluminescent assay detection method.

Supporting Information Available: General synthetic methods and procedures as well as characterization of the compounds are provided. This material is available free of charge via the Internet at http://pubs.acs.org.

References

(1) Cali, J. J.; Ma, D.; Sobol, M.; Simpson, D. J.; Frackman, S.; Good, T. D.; Daily, W. J.; Liu, D. Luminogenic cytochrome P450 assays. *Expert Opin. Drug Metab. Toxicol.* **2006**, *2*, 629–645.

(2) Cali, J. J.; Niles, A.; Valley, M. P.; O'Brien, M. A.; Riss, T. L.; Shultz, J. Bioluminescent assays for ADMET. *Expert Opin. Drug Metab. Toxicol.* **2008**, *4*, 103–120.

(3) Fan, F.; Wood, K. V. Bioluminescent assays for high-throughput screening. *Assay Drug Dev. Technol.* **2007**, *5*, 127–136.

(4) Comley, J. Kinase screening and profiling-spoilt for choice. *Drug Discovery World* **2006**, *7*, 27–50.

(5) Inglese, J.; Johnson, R. L.; Simeonov, A.; Xia, M.; Zheng, W.; Austin, C. P.; Auld, D. S. High-throughput screening assays for the identification of chemical probes. *Nat. Chem. Biol.* **2007**, *3*, 466–479.

(6) Wu, S.; Liu, B. Application of scintillation proximity assay in drug discovery. *BioDrugs* **2005**, *19*, 383–392.

(7) Sportsman, J. R.; Gaudet, E. A.; Boge, A. Immobilized metal ion affinity-based fluorescence polarization (IMAP): advances in kinase screening. *Assay Drug Dev. Technol.* **2004**, *2*, 205–214.

(8) Lowery, R. G.; Kleman-Leyer, K. Transcreener: screening enzymes involved in covalent regulation. *Expert Opin. Ther. Targets* **2006**, *10*, 179–190.

(9) Huss, K. L.; Blonigen, P. E.; Campbell, R. M. Development of a Transcreener Kinase Assay for Protein Kinase A and Demonstration of Concordance of Data with a Filter-Binding Assay Format. *J. Biomol. Screening* **2007**, *12*, 578–584.

(10) Klink, T. A.; Kleman-Leyer, K. M.; Kopp, A.; Westermeyer, T. A.; Lowery, R. G. Evaluating PI3 kinase isoforms using Transcreener ADP assays. *J. Biomol. Screening* **2008**, *13*, 476–485.

(11) Schroter, T.; Minond, D.; Weiser, A.; Dao, C.; Habel, J.; Spicer, T.; Chase, P.; Baillargeon, P.; Scampavia, L.; Schurer, S.; Chung, C.; Mader, C.; Southern, M.; Tsinoremas, N.; LoGrasso, P.; Hodder, P. Comparison of miniaturized time-resolved fluorescence resonance energy transfer and enzyme-coupled luciferase high-throughput screening assays to discover inhibitors of Rho-kinase II (ROCK-II). *J. Biomol. Screening* **2008**, *13*, 17–28.

(12) Singh, P.; Harden, B. J.; Lillywhite, B. J.; Broad, P. M. Identification of kinase inhibitors by an ATP depletion method. *Assay Drug Dev. Technol.* **2004**, *2*, 161–169.

(13) Koresawa, M.; Okabe, T. High-throughput screening with quantitation of ATP consumption: a universal non-radioisotope, homogeneous assay for protein kinase. *Assay Drug Dev. Technol.* **2004**, *2*, 153–160.

(14) Manning, G.; Whyte, D. B.; Martinez, R.; Hunter, T.; Sudarsanam, S. The protein kinase complement of the human genome. *Science* **2002**, *298*, 1912–1934.

(15) Auld, D. S.; Southall, N. T.; Jadhav, A.; Johnson, R. L.; Diller, D. J.; Simeonov, A.; Austin, C. P.; Inglese, J. Characterization of chemical libraries for luciferase inhibitory activity. *J. Med. Chem.* **2008**, *51*, 2372–2386.

(16) Auld, D. S.; Thorne, N.; Nguyen, D. T.; Inglese, J. A specific mechanism for nonspecific activation in reporter-gene assays. *ACS Chem. Biol.* **2008**, *3*, 463–470.

(17) Heitman, L. H.; van Veldhoven, J. P.; Zweemer, A. M.; Ye, K.; Brussee, J.; AP, I. J. False positives in a reporter gene assay: identification and synthesis of substituted *N*-pyridin-2-ylbenzamides as competitive inhibitors of firefly luciferase. *J. Med. Chem.* **2008**, *51*, 4724–4729.

(18) Ye, L.; Buck, L. M.; Schaeffer, H. J.; Leach, F. R. Cloning and sequencing of a cDNA for firefly luciferase from *Photuris pennsylvanica*. *Biochim. Biophys. Acta* **1997**, *1339*, 39–52.

(19) Hall, M. P.; Gruber, M. G.; Hannah, R. R.; Jennens-Clough M. L., Wood, K. V.; *Stabilization of Firefly Luciferase Using Directed Evolution*; John Wiley & Sons: New York, 1998.

(20) Varney, M. A.; Cosford, N. D.; Jachec, C.; Rao, S. P.; Sacaan, A.; Lin, F. F.; Bleicher, L.; Santori, E. M.; Flor, P. J.; Allgeier, H.; Gasparini, F.; Kuhn, R.; Hess, S. D.; Velicelebi, G.; Johnson, E. C. SIB-1757 and SIB-1893: selective, noncompetitive antagonists of metabotropic glutamate receptor type 5. *J. Pharmacol. Exp. Ther.* **1999**, *290*, 170–181.

(21) PubChem. http://pubchem.ncbi.nlm.nih.gov/.

(22) Inglese, J.; Auld, D. S.; Jadhav, A.; Johnson, R. L.; Simeonov, A.; Yasgar, A.; Zheng, W.; Austin, C. P. Quantitative high-throughput screening: A titration-based approach that efficiently identifies biological activities in large chemical libraries. *Proc. Natl. Acad. Sci. U.S.A* **2006**, *103*, 11473–11478.

(23) Yasgar, A.; Shinn, P.; Jadhav, A.; Auld, D. S.; Michael, S.; Zheng, W.; Austin, C. P.; Inglese, J.; Simeonov, A. Compound Management for Quantitative High-Throughput Screening. *J. Assoc. Lab. Autom.* **2008**, *13*, 79–89.

(24) Cleveland, P. H.; Koutz, P. J. Nanoliter dispensing for uHTS using pin tools. *Assay Drug Dev. Technol.* **2005**, *3*, 213–225.

(25) Michael, S.; Auld, D. S.; Klumpp, C.; Jadhav, A.; Zheng, W.; Thorne, N.; Austin, C. P.; Inglese, J.; Simeonov, A. A robotic platform for quantitative high-throughput screening. *Assay Drug Dev. Technol.* **2008**, *6*, 637–658.

(26) Free Software and Code for Public Use. http://www.ncgc.nih.gov/resources/software.html.

(27) Eastwood, B. J.; Farmen, M. W.; Iversen, P. W.; Craft, T. J.; Smallwood, J. K.; Garbison, K. E.; Delapp, N. W.; Smith, G. F. The minimum significant ratio: a statistical parameter to characterize the reproducibility of potency estimates from concentration−response assays and estimation by replicate-experiment studies. *J. Biomol. Screening* **2006**, *11*, 253–261.

(28) Baki, A.; Bielik, A.; Molnar, L.; Szendrei, G.; Keseru, G. M. A high throughput luminescent assay for glycogen synthase kinase-3β inhibitors. *Assay Drug Dev. Technol.* **2007**, *5*, 75–83.

(29) Wood, K. V.; Hall, M. P.; Gruber, M. G. Thermostable luciferases from *Photuris pennsylvanica* and *Pyrophorus plagiopthalamus* and methods of production Patent WO 01/20002 A1, 2001.

(30) Zhang, J. H.; Dawes, G.; Stemmer, W. P. Directed evolution of a fucosidase from a galactosidase by DNA shuffling and screening. *Proc. Natl. Acad. Sci. U.S.A.* **1997**, *94*, 4504–4509.

(31) Lembert, N. Firefly luciferase can use L-luciferin to produce light. *Biochem. J.* **1996**, *317* (Pt 1), 273–277.

(32) Nakamura, M.; Maki, S.; Amano, Y.; Ohkita, Y.; Niwa, K.; Hirano, T.; Ohmiya, Y.; Niwa, H. Firefly luciferase exhibits bimodal action depending on the luciferin chirality. *Biochem. Biophys. Res. Commun.* **2005**, *331*, 471–475.

(33) Wang, W. Q.; Xu, Q.; Shan, Y. F.; Xu, G. J. Probing local conformational changes during equilibrium unfolding of firefly luciferase: fluorescence and circular dichroism studies of single tryptophan mutants. *Biochem. Biophys. Res. Commun.* **2001**, *282*, 28–33.

(34) Rosendahl, M. S.; Leonard, N. J.; DeLuca, M. Dimensional probing of the ATP binding site on firefly luciferase. *Photochem. Photobiol.* **1985**, *35*, 857–861.

(35) Paiardini, A.; Sali, R.; Bossa, F.; Pascarella, S. "Hot cores" in proteins: comparative analysis of the apolar contact area in structures from hyper/thermophilic and mesophilic organisms. *BMC Struct. Biol.* **2008**, *8*, 14.

(36) Zavodszky, P.; Kardos, J.; Svingor Petsko, G. A. Adjustment of conformational flexibility is a key event in the thermal adaptation of proteins. *Proc. Natl. Acad. Sci. U.S.A.* **1998**, *95*, 7406–7411.

(37) Schafer, M.; Egner, U. Structural Aspects of Drugability and Selectivity of Protein Kinases in Inflammation. *Anti-Inflammatory Anti-Allergy Agents Med. Chem.* **2007**, *6*, 5–17.

(38) Schneider, M. A rational approach to maximize success rate in target discovery. *Arch. Pharm. (Weinheim)* **2004**, *337*, 625–633.

(39) Lowinger, T. B.; Riedl, B.; Dumas, J.; Smith, R. A. Design and discovery of small molecules targeting raf-1 kinase. *Curr. Pharm. Des.* **2002**, *8*, 2269–2278.

(40) Wan, P. T.; Garnett, M. J.; Roe, S. M.; Lee, S.; Niculescu-Duvaz, D.; Good, V. M.; Jones, C. M.; Marshall, C. J.; Springer, C. J.; Barford, D.; Marais, R. Mechanism of activation of the RAF-ERK signaling pathway by oncogenic mutations of B-RAF. *Cell* **2004**, *116*, 855–867.

(41) Shewchuk, L. M.; Hassell, A. M.; Ellis, B.; Holmes, W. D.; Davis, R.; Horne, E. L.; Kadwell, S. H.; McKee, D. D.; Moore, J. T. Structure of the Tie2 RTK domain: self-inhibition by the nucleotide binding loop, activation loop, and C-terminal tail. *Structure* **2000**, *8*, 1105–1113.

(42) Fabbro, D. An interview with Doriano Fabbro Ph D., Novartis Biomedical Research Institute Interviewed by Vicki Glaser. *Assay Drug Dev. Technol.* **2004**, *2*, 109–114.

(43) Egner, U.; Hillig, R. C. A structural biology view of target druggability. *Expert Opin. Drug Discovery* **2008**, *3*, 391–401.

(44) Hajduk, P. J.; Greer, J. A decade of fragment-based drug design: strategic advances and lessons learned. *Nat. Rev. Drug Discovery* **2007**, *6*, 211–219.

(45) Cheng, A. C.; Coleman, R. G.; Smyth, K. T.; Cao, Q.; Soulard, P.; Caffrey, D. R.; Salzberg, A. C.; Huang, E. S. Structure-based maximal affinity model predicts small-molecule druggability. *Nat. Biotechnol.* **2007**, *25*, 71–75.

(46) Hopkins, A. L.; Groom, C. R. The druggable genome. *Nat. Rev. Drug Discovery* **2002**, *1*, 727–730.

(47) Schurer, S. C.; Brown, S. J.; Gonzalez-Cabrera, P. J.; Schaeffer, M. T.; Chapman, J.; Jo, E.; Chase, P.; Spicer, T.; Hodder, P.; Rosen, H. Ligand-binding pocket shape differences between sphingosine 1-phosphate (S1P) receptors S1P1 and S1P3 determine efficiency of chemical probe identification by ultrahigh-throughput screening. *ACS Chem. Biol.* **2008**, *3*, 486–498.